Analytica Chimica Acta 1227 (2022) 340257

Contents lists available at ScienceDirect

Analytica Chimica Acta

journal homepage: www.elsevier.com/locate/aca

A fully handwritten-on-paper copper nanoparticle ink-based electroanalytical sweat glucose biosensor fabricated using dual-step pencil and pen approach

Amarprit Singh [a,*], Anil Hazarika [b], Lachit Dutta [c], Abhishruti Bhuyan [d], Manabendra Bhuyan [a]

[a] Department of Electronics and Communication Engineering, Tezpur University, Tezpur, 784028, Assam, India
[b] Department of Physics, Cotton University, Guwahati, 781001, Assam, India
[c] Department of Electronics and Communication Engineering, Gauhati University, Guwahati, 781014, Assam, India
[d] Department of Electronics and Communication Engineering, Regional Institute of Science and Technology, Ri-Bhoi, 793101, Meghalaya, India

HIGHLIGHTS

- Sensor is fabricated by hand drawing a layer of copper nanoparticle ink over pencil-drawn electrode (PDE).
- Ink deposition allows permeation of glucose sensitive copper nanoparticles.
- CuNP-ink/PDE is composed of 44.5% of metallic Cu nanoparticles.
- Sensor offers sensitivity of 2616.6 μA mM^{-1} cm^{-2} and detection limit of 0.5 μM.
- Results are compared with UV–Vis spectrophotometric assay in real sweat samples.

GRAPHICAL ABSTRACT

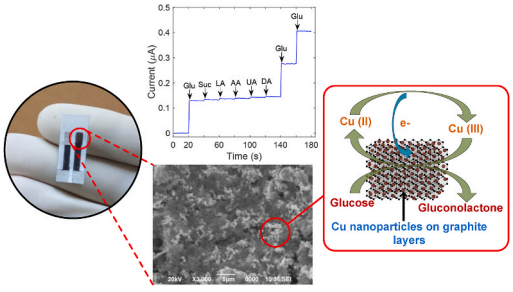

ARTICLE INFO

Keywords:
Paper-based sensor
Glucose sensing
Pencil-drawn electrodes
Hand-drawn sensing layer
Copper nanoparticle ink

ABSTRACT

This article reports a facile fabrication of a highly sensitive enzyme-free sweat glucose sensor over Whatman filter paper substrate employing a dual-step pencil and pen approach. Initially, two pencil-drawn electrodes (PDEs) are obtained on the filter paper through the manual abrasion of an 8B graphite pencil. Then, the sensing layer is drawn over one of the PDEs using a custom-made copper (Cu) nanoparticle ink (CuNP-ink) pen to form copper nanoparticle ink decorated PDE (CuNP-ink/PDE) which serves as a working electrode, while the other PDE is drawn with silver conductive ink (Ag-ink) pen to form reference electrode. The developed CuNP-ink/PDE is composed of 43.5% of metallic Cu nanoparticles, inducing a highly crystalline and conductive nature, thus promoting fast electron transfer during glucose electrooxidation. The developed sensor offers a sensitivity of 2691.7 $\mu AmM^{-1}cm^{-2}$, a detection limit of 0.5 μM, a linear range of 1.2–40 μM, and a fast response time of ~ 1.5 s. Besides, the sensor measurements are stable, reproducible, and selective in glucose sensing. Also, the reliability of the sensor is tested by comparing its performance with a UV–Visible spectrophotometer for proving its efficacy in sweat glucose detection. Experimental results evince the effectiveness of the designed sensor for glucose detection in human sweat.

* Corresponding author.
E-mail addresses: singhamarprit21@gmail.com (A. Singh), anilhazarika8@gmail.com (A. Hazarika), lachitdutta@gmail.com (L. Dutta), abhishruti29@gmail.com (A. Bhuyan), manab@tezu.ernet.in (M. Bhuyan).

https://doi.org/10.1016/j.aca.2022.340257
Received 22 May 2022; Received in revised form 9 August 2022; Accepted 10 August 2022
Available online 27 August 2022
0003-2670/© 2022 Elsevier B.V. All rights reserved.

1. Introduction

Diabetes mellitus has been emerging as the most severe form of chronic epidemic across the globe [1,2]. A study conducted by International Diabetes Federation (IDF) estimated that approximately 194 million people across the globe, or 5.1% in the adult population, have diabetes and this number is projected to hike up to 333 million, or 6.3%, by 2025 [3]. It is a well-known fact that the root cause of diabetes mellitus is linked with uncontrolled regulation of glucose levels in the body [4]. Therefore, frequent monitoring of glucose is vital for the prevention of fatal health problems such as cardiovascular and kidney diseases, strokes, blindness, neuropathy, etc. [5–7]. Conventional method for glucose assessment employs an invasive finger-pricking procedure for blood extraction which is painful and inconvenient to the patient [8]. Besides, the use of sophisticated laboratory equipment and the involvement of trained laboratory personnel [7] for quantifying blood glucose further limits the traditional approach and exerts a high-cost burden on the population. In such cases, assessments ensuring non-invasive, low-cost, and effective glucose detection utilizing biofluids such as sweat is the most demandable [9,10]. Also, a strong correlation between glucose levels in blood and sweat further permits the use of sweat as an alternative biofluid for continuous tracking of glucose levels for the prevention of diabetes mellitus [11]. Thus, sweat offers a low-cost and reliable means of glucose detection for improving patients' health.

Sweat is an important biological fluid easily accessible from the body. It has rich contents of biomarkers including biomolecules (ascorbic, uric acid, etc.), metabolites (glucose, urea, etc.), electrolytes (Na^+, K^+, Cl^-, etc.), and proteins [12] that provide relevant physiological information regarding individual health fitness. Thus, the assessment of sweat glucose provides a continuous track of diabetes and proper management of other associated health risks [13]. Recently, the advancements in sweat-based electroanalytical sensing technologies have enabled the design and development of flexible sensing platforms for accurate detection of glucose [14,15]. Moreover, due to the ease of non-invasive collection, sweat-based electrochemical techniques are getting wider attention for developing reliable and affordable glucose sensors with excellent selectivity, high sensitivity, and rapid response time. For instance, Gao et al. [16] track the metabolites and electrolytes in human sweat using a wearable patch. Wang et al. [6] employed sweat for glucose detection using a thin-film polyethylene terephthalate electrochemical biosensor. Besides, other glucose sensors include iontophoresis-based skin interstitial fluid sensor [17], and epidermal electrochemical-based sensor [18] for sweat glucose monitoring through proper harvesting and treatment [11]. Despite the consistent performance, such sensors suffer challenges due to their low concentration volume which necessitates the use of highly sensitive techniques for glucose evaluation.

The effectiveness of the sensor depends on the choice of the proper substrate. Typical flexible substrates used in non-invasive biosensors such as polyethylene terephthalate [19], polyimide [20], polydimethylsiloxane [21], polyurethane [22] and polymethyl methacrylate [23] accumulate sweat and provides inaccurate detection of biomarkers due to the mismatch between substrates and epidermis [24]. To address such an issue, Whitesides et al. [25] introduced the first Paper-based Analytical Devices adopting cellulose paper substrate. Such substrates offer absorption and dispersion of sweat owing to its inherent capillary action, thus facilitating the analysis of low volume samples [26]. Moreover, paper substrate enables fabrication of microfluidic channels through hydrophilic and hydrophobic process [27], inkjet printing [28], wax printing [29] and photolithography [30]. Another inherent characteristic of the paper substrate is softness and foldability that provides ease of fabrication in getting simplified and cost-effective testing probe [31]. Besides, the roughness of the paper is a crucial parameter for fabricating pencil-drawn electrodes (PDEs) [32]. Due to high roughness between 1 and 5 μm [33], Whatman filter paper serves as a suitable substrate for the pencil-drawn electrode, thus, promoting exfoliation of the pencil graphite rod for the deposition of continuous conductive graphite layers [34] with optimal electrical conductivity [35]. The process of direct writing on paper is advantageous since the sensitive material layer can be directly deposited by simple abrasion of graphite pencil on the paper substrate for getting simplified and cost-effective sensing probes [32]. Therefore, with researchers continuously exploring new electrode fabrication techniques, the focus has turned towards hand-drawn PDEs, where one can draw their electrode contributing to an extremely economical approach to producing electrochemical sensing platforms [36,37].

Non-enzymatic glucose sensors employing metal nanoparticle or carbon nanomaterial-based electrodes outweigh the challenges suffered by their enzymatic counterpart [38,39]. Enzymatic sensors employing glucose oxidase (Gox) offer good sensitivity and selectivity but suffer various limitations including lower life span, cost of the enzyme, poor stability, complex immobilization technique [40]. Also, the effect of pH, temperature, toxic chemicals, and humidity highly degrades the performance of Gox [41]. Recently, non-enzymatic glucose sensors employing metal alloys [42], metal nanoparticles [43], metal oxides [44], are gaining wide attention due to their outstanding electrocatalytic properties. Moreover, the advent of carbon nanomaterials such as graphene [45], carbon nanotube [46], etc. has further reformed sensor technology in terms of economy and ease of fabrication [47]. Numerous paper-based sensors employing copper-carbon and copper oxide-carbon amalgamation for fabricating non-enzymatic glucose sensors are reported [48,49]. Copper (Cu) nanomaterial promotes better electron transfer at low potential and greatly enhances glucose oxidation due to the electrocatalytic effect of Cu(II)/Cu(III) redox couple in a strong alkaline medium [50]. Moreover, Cu nanostructures have gained exceptional consideration due to their low bandgap energies (1.4–2.3 eV), excellent catalytic activity, low overpotential, biocompatibility, and affordability [51]. As such, Wang et al. [48] developed a flexible and electrochemical sweat platform by depositing Cu submicron buds on freestanding graphene paper (GP) carrying MoS_2 nanocrystals monolayer for bio-functional detection of glucose and lactate. Prabhakaran et al. [49] developed a nonenzymatic glucose sensor by engineering the surface of laser scribed graphene (LSG) by conformal anchoring of copper oxide nanoparticles (CuO NPs). Janmee et al. [52] reported a non-enzymatic electrochemical sensor fabrication using a nanocomposite of copper oxide nanoparticles, ionic liquid and reduced graphene oxide (CuO-IL/rGO) modified on the screen-printed carbon electrode (SPCE) for glucose determination in human urine and electrolyte drinks. Yang et al. [53] developed a disposable non-enzymatic glucose sensor utilizing a three-dimensional graphene wall (GWs) and nano-Cu_2O modified carbon fiber paper (CFP) electrode. However, in the aforesaid works, the reduction of graphene oxide and its surface modification are the two steps involved in the fabrication of graphene-based copper nanocomposite electrodes. Furthermore, the fabrication process involved tedious complex synthesis steps, the need for volatile solvents, high temperature, a large volume of contaminant residues, etc. [54]. This urges the necessity of a facile and green approach toward the deposition of catalytic material on the electrode surface for the construction of a glucose biosensor.

In this article, we have presented a very simple and efficient way of developing a glucose sensor by depositing the sensing layer through a dual-step writing process with a pencil and pen on the Whatman filter paper substrate. An 8B pencil is used to deposit two pencil-drawn electrodes (PDE) of which one of the PDEs is drawn with a sensing layer of copper nanoparticle ink (CuNP-ink) using a custom-made pen that serves as a working electrode and the other PDE is drawn with a silver conductive ink pen to form reference electrode. The ink deposition allows the permeation of glucose-sensitive copper nanoparticles deep into the porous paper fiber. Moreover, the large surface area of metallic nano copper allows faster electrooxidation of glucose in a strongly alkaline medium. Electrochemical characterization using cyclic

voltammetry (CV) and chronoamperometry (i-t) reveals a high sensing ability of deposited CuNP-ink in glucose ambiance. Results of the developed sensor are compared with a UV–Visible spectrophotometer to prove the reliability of the sensor in evaluating real sweat samples. To the best of our knowledge, such fabrication of a non-enzymatic glucose sensor using a custom-made pen loaded with synthesized CuNP-ink employing a hand-drawn technique of electrocatalytic material deposition has not been reported so far.

2. Materials and methods

2.1. Chemicals and materials

All the chemicals purchased and used are of ACS grade and used without further purification. D-glucose anhydrous ($C_6H_{12}O_6$), ascorbic acid ($C_6H_8O_6$), uric acid ($C_5H_4N_4O_3$), dopamine ($C_8H_{11}NO_2$), sucrose ($C_{12}H_{22}O_{11}$), and lactic acid ($C_3H_6O_3$) are purchased from Sigma-Aldrich. De-ionized (DI) water used for the preparation of stock solutions is obtained from the Millipore Milli-Q purification system (Synergy UV system). Stock solutions of D-glucose and sodium hydroxide are prepared using DI water (> 18 MΩ). Silver conductive ink pen (842AR-P), paraffin wax, filter paper (Whatman^{TM} Grade 3MM CHR), epoxy adhesive, sodium hydroxide (NaOH), copper chloride ($CuCl_2$), sodium citrate ($Na_3C_6H_5O_7$), and sodium formaldehyde sulfoxylate (CH_3NaO_3S) are purchased from Thermo Fisher Scientific, India. High-quality Apsara Assorted drawing pencils grades (1B, 2B, 3B, 4B, 5B, 6B, 8B, 10B, and 12B) are purchased from Amazon, India.

2.2. Measurement and instrumentation

Bulk resistance of PDEs is measured with a precise multimeter (KEITHLEY 2110 $5\frac{1}{2}$ Digit Multimeter) and the square resistance of the PDEs on the Whatman filter paper substrate is measured using the four-probe method. A digital dynamometer (EMB-02) is used to calibrate the handwriting force during the fabrication of PDEs. Scanning electron microscopy (SEM) and energy-dispersive X-ray (EDX) spectroscopy are achieved through a JEOL JSM 6390LV SEM (accelerating voltage range: 0.5 kV − 30 kV). X-ray Diffraction (XRD) profiles of CuNP-ink/PDE are observed with Powder XRD (D8 FOCUS), BRUKER AXS, GERMANY, employing high-intensity Cu Kα radiation. Precise weight measurement of analytes is done in Aczet CY205C Semi-Micro Balance and the solutions are made under constant stirring. A BioLogic (SP-300) potentiostat-galvanostat is employed to perform cyclic voltammetry and amperometric measurements. The SP-300 device is configured as a two-electrode system for measurements with the fabricated two-electrode sensor (see Supplementary Information, Section S1). In a two-electrode system, the current and sensing leads are connected i.e., Working (W) and Working Sense (WS) leads are connected to a working electrode, and Reference (R) and the Counter (C) leads are connected to a second (aux, counter, or quasi-/pseudo reference) electrode as shown in Fig. S1(a) and Fig. 1d. Thus, the sense leads measure whole-cell voltage i.e., the complete voltage dropped by the current flowing across the whole electrochemical cell; the working electrode, electrolyte, and the counter/reference electrode (see Supplementary Information, Section S1.1). A UV–Visible Spectrophotometer (SHIMADZU UV-2450) is employed to assure the trueness of the glucose levels measured by the fabricated sensor in sweat samples. Besides, all software data processing is done in MATLAB R2015a (Ver. 8.5.0).

2.3. Synthesis of copper nanoparticles

The method of copper nanoparticles synthesized is obtained from reported literature [55]. Copper chloride solution is prepared by adding 5 g of copper chloride in 100 mL de-ionized (DI) water and mixed with sodium citrate solution to maintain a ratio of 1:5. After 30 min, an aqueous solution of sodium formaldehyde sulfoxylate is added to the mixture at a 1:1 ratio with respect to copper chloride with continuous stirring at room temperature. The solution is further stirred for 1 h at 55 °C resulting in a brown precipitate of copper nanoparticles which is centrifuged, collected, washed with DI water, and dried in a vacuum for 3 h.

2.4. Preparation of ink and pen

To obtain CuNP-ink, initially, 3 g of synthesized Cu nanoparticle is added to 5 mL of purchased carbon conductive ink (Fig. S2) and is subjected to sonication for 30 min. Then 5 mL of DI water and 2 mL of epoxy adhesive is added and further sonicated for 45 min. Thereafter, the ink is poured into an empty syringe and kept for 12 h before use.

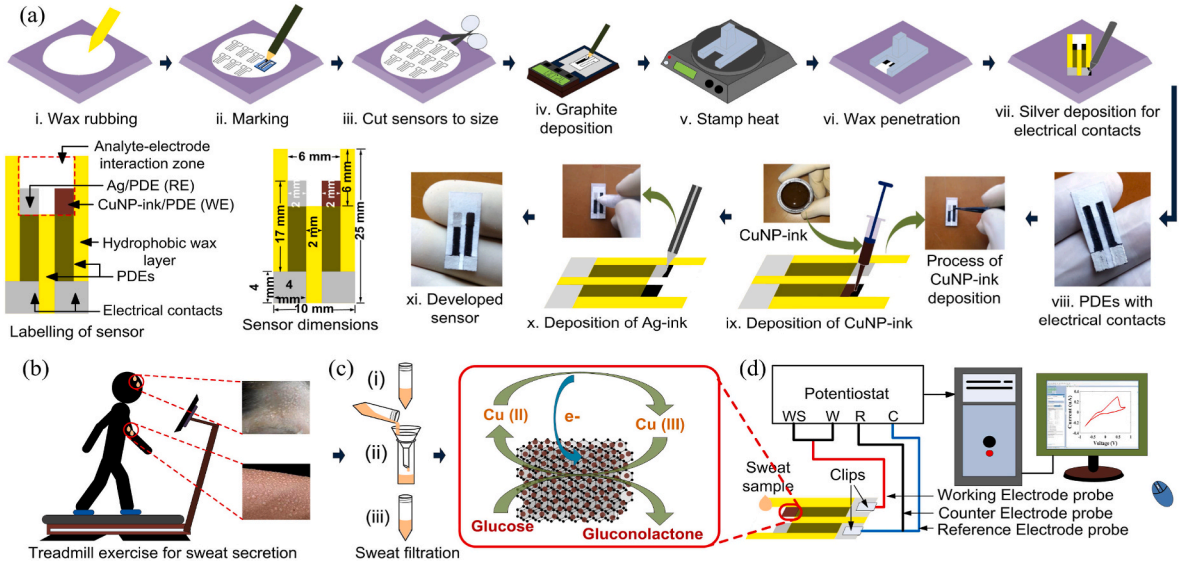

Fig. 1. (a) Design and fabrication of two-electrode non-enzymatic sweat glucose sensor (step: i-xi) along with the sensor dimensions and labelling, (b) sweat generation during physical activity inside a gymnasium room at room temperature, (c) sweat filtration, and (d) measurement set-up showing the developed sensor connected to a potentiostat interfaced with a computer for determination of sweat glucose level in a sweat sample.

2.5. Fabrication of glucose sensor

Fig. 1a shows the complete fabrication process of the sensor developed by hand drawing on Whatman filter paper substrate. Initially, one side of the paper is rubbed with dry wax. Then, a 3D printed stencil made of polylactic acid (PLA), designed in AutoCAD, is directly placed on the paper substrate with wax side downwards and outlines of the PDEs are drawn. The paper is then cut into a dimension of 25 mm × 10 mm with the drawn outlines and placed over a digital dynamometer to calibrate the writing force for uniform graphite deposition with optimal conductivity for each PDE. An 8B pencil is used to deposit the graphite layers within the empty spaces provided for electrodes by writing seventy times with an applied force of ~0.7–0.9 N. A 3D printed PLA stamp is heated to 50 °C and placed over the paper substrate with PDEs for 10 s for the wax to penetrate the substrate. However, an area of 2 mm × 2 mm on the top of both PDEs is left unwaxed so that the inks can penetrate the porous paper surface. Electrical contacts are made with a silver ink pen for connecting the sensor to an external circuit for measurements. To deposit the sensing layer, the custom-made CuNP-ink pen is oriented over one of the PDEs and an ink trace is drawn on it. The other PDE is drawn over with silver conductive ink to facilitate free electron transfer during electro-oxidation of glucose. The physical dimension and labeling of different regions of the fabricated sensor are shown in Fig. 1a.

3. Results and discussion

3.1. Selection of pencil grade

Pencil graphite lead exhibits different physical properties because of its composition. The pencil lead is composed of graphite, clay, and a minute amount of wax; wherein the wax forms the binder for the lead. Commercial pencils are classified in terms of H and B grades respectively depending on the graphite-to-clay ratio. The grade H stands for hardness arising from higher clay content and the latter stands for blackness which is because of higher graphite content. For drawing the electrodes, the selection of pencils is made from available pencil grades of 6H to 12B. However, as the need for greater conductivity is a priority for fabricating the PDE, pencil grades from 1B to 12B are considered, and accordingly, the conductivity of pencil leads and square resistance of the electrodes fabricated on Whatman filter paper are investigated as shown in Table 1. As observed, the bulk conductance of the pencil lead increases with the graphite content but shows an insignificant difference among the graphite content of higher pencil grades. Also, it is revealed that the square resistance of the PDE fabricated using an 8B pencil is the least among all the pencil grades. Therefore, an 8B graphite pencil is selected for fabricating PDE for all the sensors.

3.2. Structural characterization

Fig. 2a displays the SEM image of PDE which reveals non-uniform graphite traces throughout the electrode due to manual abrasion of the 8B graphite pencil. The presence of uneven clusters of graphite flakes corroborates the successful deposition of graphite layers on the paper substrate. Moreover, the formation of hydrophobic wax boundary and distinct graphite trace over the paper substrate can also be seen clearly (Fig. S3). In Fig. 2b, the accumulation of dense silver wrinkles on the surface of the PDE assure the formation of Ag/PDE. Further, the SEM image of CuNP-ink/PDE (Fig. 2c) shows the accumulation of tiny grain-like Cu nanoparticles. The nanoparticles are uniformly distributed over the PDE surface which assures enhanced sensing performance of the hand-drawn electrode.

Table 1
Conductance of different pencil grade leads and square resistance of the pencil trace on Whatman filter paper.

Pencil grades	Conductivity ($\times 10^3$) (S/m)	Square resistance (Ω)
1B	2.45	7869
2B	2.85	5856
3B	2.92	3814
4B	3.11	1017
5B	3.23	469
6B	3.31	315
8B	3.35	287
10B	3.38	385
12B	3.41	566

As shown in Fig. 2d (i), EDX analysis affirms the purity of the Ag ink in Ag/PDE wherein no specific trace of oxygen is observed. This is because the silver ink used in the fabrication of Ad/PDE is water resistant [56] (Table S3). However, a small carbon peak in the spectrum is due to the presence of the graphite layer below the deposited silver ink. Moreover, the EDX spectrum of the CuNP-ink/PDE reveals the presence of 44.5% of metallic Cu nanoparticles in the deposited CuNP-ink. However, the occurrence of carbon and oxygen further affirms the composition of fabricated CuNP-ink/PDE (Fig. 2d (ii)). It is noteworthy that the traces of oxygen appears in the CuNP-ink due to the presence of water molecules contributed by the de-ionized water used in the process of synthesizing the ink. Fig. 2e and f shows the XRD pattern of Ag/PDE and CuNP-ink/PDE respectively. Four major peaks are seen in the case of Ag/PDE at 38.32^o, 44.50^o, 64.61^o, 77.54^o for 2θ which correspond to the diffraction planes (111), (200), (220), and (311) of face-centered cubic Ag crystal (JCPDS 04–0783). Also, the XRD pattern for CuNP-ink/PDE (Fig. 2f) indicates a high degree of purity of the Cu nanoparticles as evident from the diffraction peaks observed at 43.30^o, 50.43^o, and 74.13^o. These peaks perfectly match with (111), (200), and (220) diffraction planes of the cubic phase of Cu (0) respectively. Notably, the purity of the nano copper is further supported by the fact that the formation of Cu_2O can be almost avoided and phase pure copper nanoparticles can be effectively synthesized by use of carboxylic acids or their salts e.g. trisodium citrate and myristic acid by use of SFS as a reducing agent [55]. This methodology is adopted in the synthesis of nano copper in this work.

To evaluate the crystallinity of the synthesized Cu nanoparticles, the average particle size of the Cu nanoparticle crystals is calculated using the Scherrer formula, $D = K\lambda/\beta cos\theta$, where D is the crystallite size, K denotes the shape factor usually taken as 0.89, λ denotes the wavelength of the X-ray radiation ($\lambda = 0.15406$ nm) for Cu Kα, and β is the full-width at half-maximum (FWHM) of the main peak. As shown in Table S4, the calculated sizes of nanocrystals are found to be 12.29 nm, 11.78 nm, and 11.90 nm respectively. Therefore, the average crystal size of Cu nanoparticles is obtained as ~ 12 nm.

3.3. Electrocatalysis of glucose at CuNP-ink/PDE

The electrocatalytic behavior of the bare PDE and CuNP-ink/PDE is studied by performing cyclic voltammetry (CV) within a potential window of −0.8V to +0.8V in 0.1 M NaOH with and without 1 mM glucose at a scan rate of 50 mV/s. It is worthwhile to mention that, before CV experimentation, the spillover limit of the analyte-electrode interaction zone (Fig. 1a, Labelling of sensor) is tested, and is found that the optimal volume of solution contained in the analyte-electrode interaction zone is 100 μL which we consider as the volume of the electrochemical cell. As evident from Fig. 4a, the absence of glucose does not produce any oxidation peak for both PDE and CuNP-ink/PDE in the observed potential window. However, a high increase of anodic current beyond +0.42 V for CuNP-ink/PDE, in absence of glucose, is attributed to the hydrolysis of the water molecule [57]. Again, no oxidation peak is observed for PDE with 1 mM glucose addition as is expected (Fig. 3a). Conversely, with the addition of 1 mM glucose, during the anodic scan, the CuNP-ink/PDE offers a broad shoulder anodic peak between −0.5 V and −0.2 V due to the synergistic effect of two phenomena: (i) Cu(0)/Cu(I) avert the interaction between Cu(0) and glucose, and (ii) the conversion of Cu(0) to Cu(II) due to the

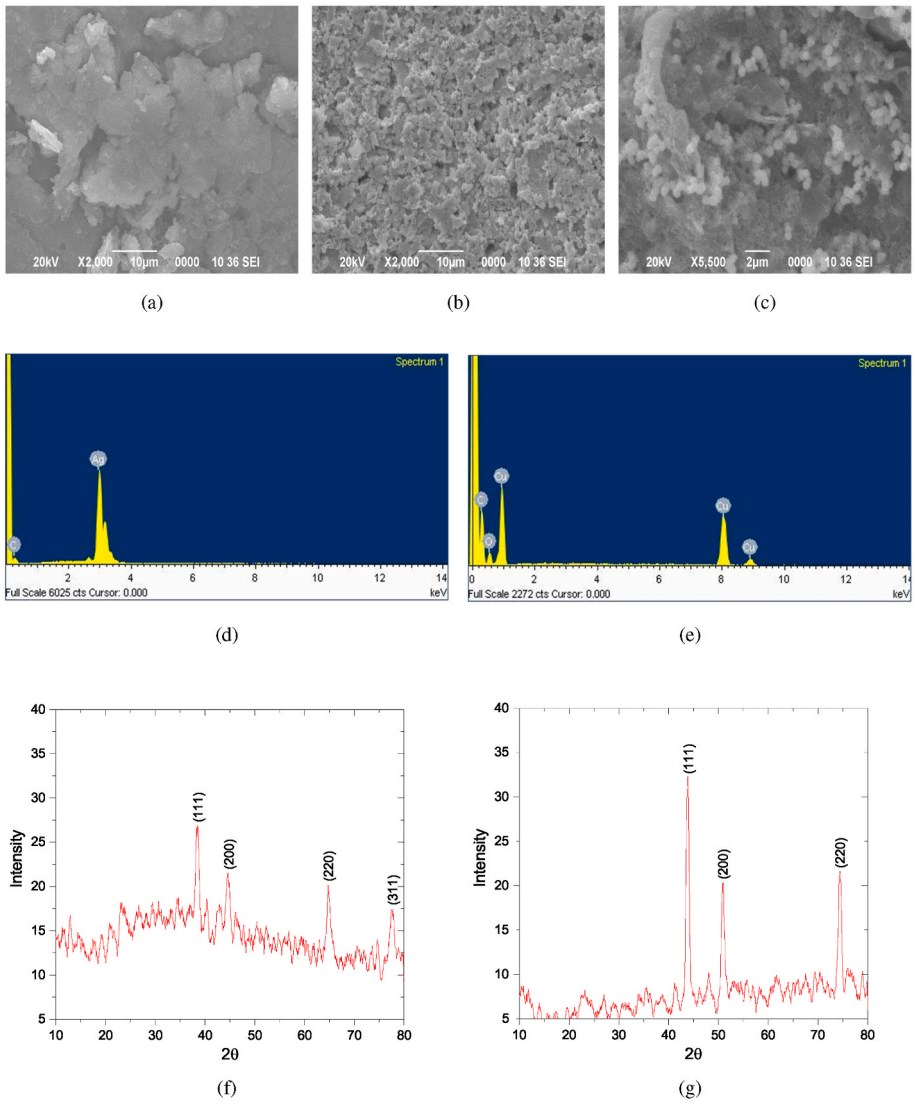

Fig. 2. Structural characterization of the electrodes. (a), (b) and (c) SEM images of PDE, Ag/PDE and CuNP-ink/PDE; (d) EDX spectrum of (i) Ag/PDE, and (ii) CuNP-ink/PDE; (e) and (f) XRD profiles of Ag/PDE and CuNP-ink/PDE.

formation of Cu(I)–glucose complex at −0.2 V [58,59]. In addition to that, a sharp oxidation peak at +0.32 V is considered to be the result of the desorption of glucose as a result of the Cu(I)/Cu(II) transition followed by a long oxide back-end beyond +0.42 V is characterized by the electrooxidation of glucose where Cu(III) and hydroxyl radicals are probably involved [58]. During the cathodic scan, from +0.8 V to 0 V, the absence of any peak indicates that Cu(III) is consumed in the electrooxidation of glucose [58]. However, the appearance of a weak bump at around −0.1 V corresponds to Cu(II)/Cu(I) transition and decreasing Cu(I)/Cu(0) transition which is hypothetically because of Cu(I)-glucose interaction [59]. Thus, the above analysis provides an elaborated scenario of the CuNP-ink-catalyzed electrooxidation of glucose in an alkaline medium.

Fig. 3b shows the effect of different scan rates on the oxidation of glucose at the CuNP-ink/PDE in 0.1 M NaOH. It is observed that the oxidation peak current rises as the scan rate increases from 10 mV/s to 150 mV/s along with a gradual shift in the peak towards higher potential because higher scan rates lead to a slower electrocatalytic reaction within the glucose molecule adsorption [60]. The linear dependency of anodic peak current (Ipa) on scan rate (v) is examined by linear regression analysis as $I_{pa} = 0.00103v + 0.079$ ($R^2 = 0.9987$) (Fig. 3c). This linear relationship reveals the occurrence of an irreversible adsorption-controlled electrochemical process on glucose electro-oxidation [61]. Also, the relation between anodic peak current (I_{pa}) and $v^{1/2}$ (inset of Fig. 3c) is found to be non-linear and is defined by second-order power equation $I_{pa} = 0.00097v^{2.02} + 0.08$ ($R^2 = 0.9987$) which further indicates that electrocatalytic oxidation of glucose at CuNP-ink/PDE is a surface-controlled irreversible reaction [61]. Furthermore, the changes in the anodic peak current with varying glucose concentrations are also examined (Fig. 3d). It is seen that on increasing the glucose concentration from 0.15 mM to 5 mM, the anodic peak current rises rapidly. This is because increasing glucose concentration accelerates the electrocatalytic reaction at the CuNP-ink/PDE, thus generating more free electrons (Fig. 1d), resulting in increasing anodic current. Moreover, with increasing glucose concentration, the oxidation peak gets shifted with the positive potential due to the increase of glucose molecules on the electrode's surface [40]. This phenomenon can be termed as potential shift. These results indicate outstanding sensing ability of CuNP-ink/PDE and, therefore, promote superior electrocatalytic performance in glucose ambiance.

3.4. Amperometric response of the CuNP-ink/PDE sensor towards glucose

One predominating factor exerted upon the amperometric response

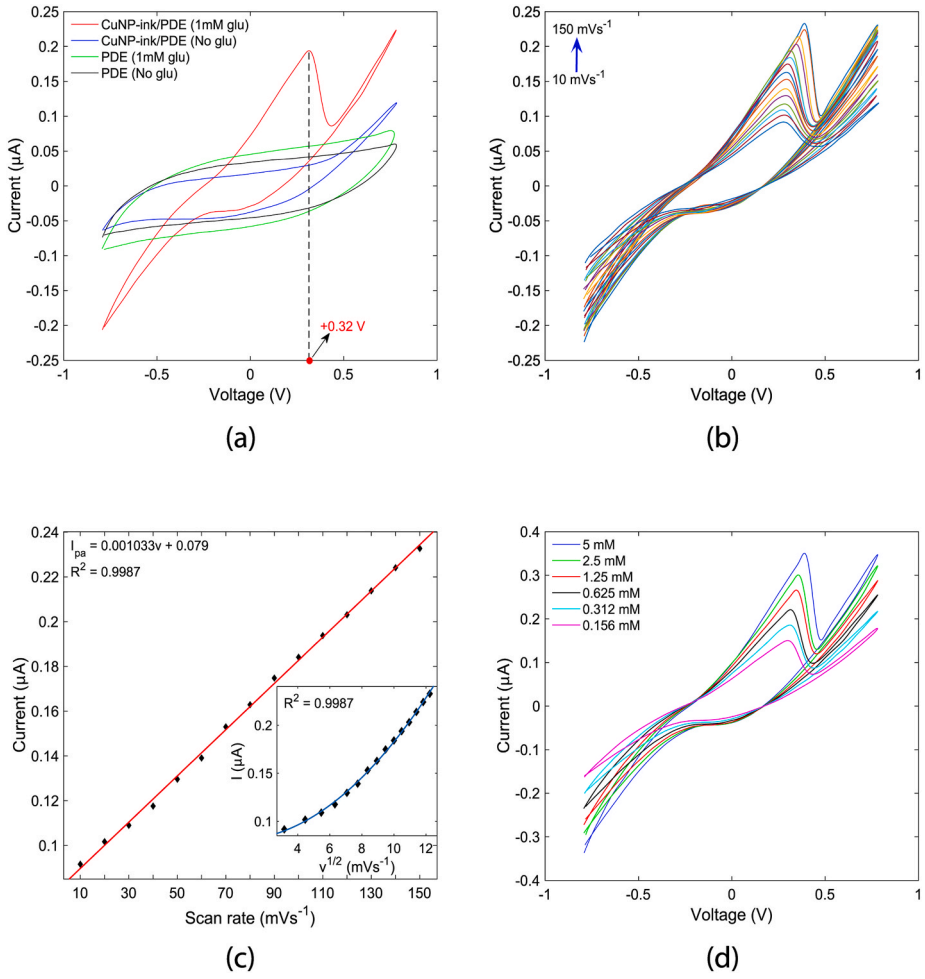

Fig. 3. (a) Cyclic voltammograms recorded on PDE and CuNP-ink/PDE in the absence and presence of 1 mM glucose in 0.1 M NaOH at a scan rate of 50 mV/s, (b) cyclic voltammograms for CuNP-ink/PDE in 0.1 M NaOH containing 0.1mM glucose at various scan rates, (c) plot of anodic peak currents (I_{pa}) vs. scan rate (v), and (d) effect of different concentrations of glucose on CuNP-ink/PDE in 0.1 M NaOH at a scan rate of 50 mV/s.

of a sensor is the impact of detection potential. Here, the optimal detection potential for the sensor is examined with a voltage range of +0.15 V to +0.35 V with the dropwise addition of 2 μL of 0.1 mM of glucose in 0.1 M NaOH. In particular, it has been observed that at high glucose concentrations, the potential is shifted slightly to more positive values (Fig. 3d). Therefore, the optimal potential detection experiment is conducted with a low glucose concentration i.e., 0.1 mM glucose. As shown in Fig. 4a, on increasing the potential from +0.15 V to +0.35 V, the currents obtained with CuNP-ink/PDE increases and reach their maximum at + 0.30 V. Therefore, avoiding the risk that any unwanted species present in sweat may get oxidized at potentials higher than +0.30 V, the optimal detecting potential selected for the sensor is +0.30 V. Furthermore, it is observed that a simple PDE produces an insignificant current response upon subsequent addition of glucose at an optimal detection potential of +0.30 V, which gives us a clear implication that the bare PDE is insensitive to glucose.

Amperometry involves the measurement of current with respect to time (i-t) at constant applied voltage. The amperometric response of the CuNP-ink/PDE and bare PDE for varying glucose concentrations (1.2 μM–5 mM) in 0.1 M NaOH is shown in Fig. 4b. As seen, at + 0.30 V, the PDE shows a negligible current response with consecutive addition of glucose aliquots of individual concentration, whereas the CuNP-ink/PDE yields a remarkably larger response. The CuNP-ink/PDE produces a distinct and stable amperometric response at + 0.30 V with consecutive drop-wise addition of 2 μL of individual concentration of glucose at 20 s intervals. Besides, the performance of CuNP-ink/PDE in the electrooxidation of glucose is also reflected by its fast response time. Fig. 4c presents the magnified view of the one-step addition of glucose and shows the response time of CuNP-ink/PDE. It has been observed that CuNP-ink/PDE responds immediately after glucose addition and the time taken to achieve 96% of the steady-state current is ~ 1.5 s, which interprets an extraordinary fast response towards glucose. The calibration curve from the amperometric responses ($n = 3$) is shown in Fig. 4d. Apparently, the CuNP-ink/PDE gives a linear response up to 40 μM (inset of Fig. 4d), beyond which a saturated response is observed for higher glucose concentration. The linear response is fitted by regression equation $y = (1.979 \pm 0.0993)x + (0.0139 \pm 0.0014)$, where y is the response current (μA) and x is the glucose concentration (mM). The linear regression (R^2) and slope (m) is obtained as 0.9850 and 2.078 (considering $m = 1.979 + 0.0993$) respectively. Therefore, the calculated sensitivity of the sensor is 2691.7 μAmM^{-1} cm^{-2} at an active sensing area of 0.000772 cm^2. The sensitivity (S) of the developed sensor is calculated using Eq. (1) [62] given below;

$$S = \frac{Slopeofcalibrationplot, m(\mu AmM^{-1})}{Activesurfacearea, A(cm^2)} \quad (1)$$

Also, the limit of detection (LOD) of the sensor is found to be 0.5 μM as calculated using $LOD = 3\sigma/S(signal/noise = 3)$, where σ denotes the standard deviation of the linear response calculated using regression analysis (see Supplementary Information, Section S2) and S is the slope of the linear region of the calibration curve. The reason for this superior performance is attributed to (i) the indispensable nanostructure of the

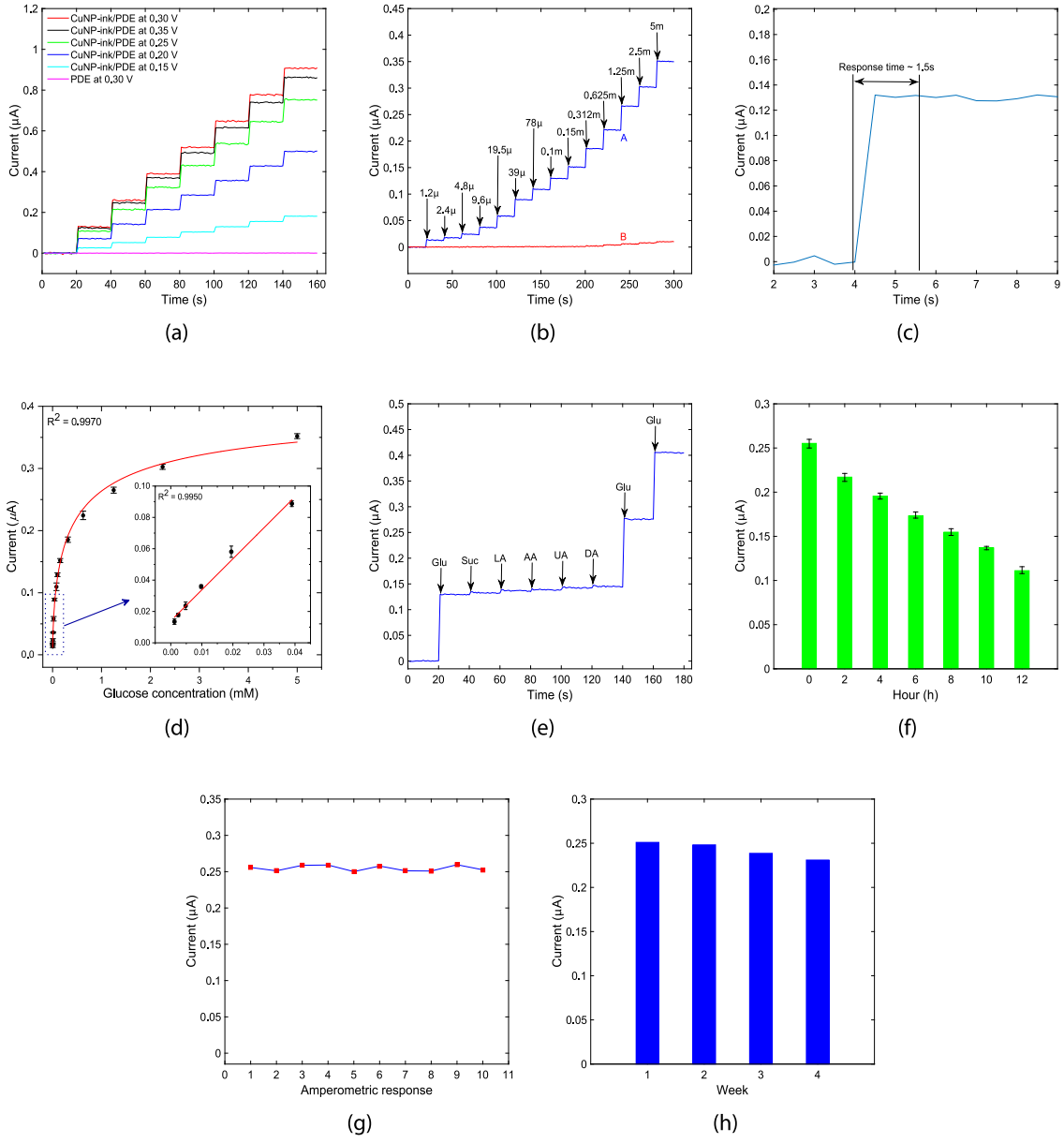

Fig. 4. (a) Investigation of optimal detection potential by studying amperometric responses of CuNP-ink/PDE at different potentials with successive addition of 0.1 mM glucose in 0.1 M NaOH, (b) amperometric response of CuNP-ink/PDE in 0.1 M NaOH with different glucose concentrations, (c) response time of CuNP-ink/PDE, (d) calibration curve obtained from the amperometric response ($n = 3$) (inset shows the linear region from 1.2 μM to 40 μM), (e) selectivity study of the developed sensor at +0.30 V with 0.1 mM glucose (Glu) in presence of various other interfering species (Suc - sucrose, LA - lactic acid, AA - ascorbic acid, UA - uric acid, DA - dopamine), (f) repeatability test of the sensor with successive addition of 1 mM glucose with an interval of 2 h, (g) reproducibility study with amperometric measurements of ten replicate sensors, and (h) shelf-life of sensor investigated with four sensors for 4 weeks.

metallic Cu that confers excellent electrical conductivity due to a larger effective surface area, thereby affording a prominent electron transfer rate at the electrode-analyte interface, and (ii) the pencil traces contains multilayer graphene and a little amount of single-layer graphene with large portion of edge-like structures [63]. These graphene layers experience morphological defects such as dislocations, edge, and edge-like defects, etc. which, again, play a significant role in the electron transfer process thus improving the performance of sensor [64]. Table 2 shows the performance comparison of the developed sensor with existing published works on paper-based non-enzymatic glucose sensors.

To analyze the applicability of the developed sensor in the real samples, wherein the sweat glucose concentration ranges from 0.2 mM to 0.6 mM [38], Langmuir-Freundlich isotherm theory [65], $I = NaC^m/(1 + aC^m)$, is used to fit the calibration curve ($n = 3$) as the oxidation of glucose on CuNP-ink/PDE is a surface catalytic process [58]; where I is the current (μA), N denotes the total number of binding sites on CuNP-ink/PDE, a is related to the median the binding affinity constant, C is glucose concentration (mM), and m is the heterogeneity index. The subsequent fitting equation (with $n = 3$) for the sensor is obtained as, $I = (0.4185 \pm 0.0199) \times (1.7 \pm 0.2417) \times C^{(0.3963 \pm 0.0250)}/(1 + (1.7 \pm 0.2417) \times C^{(0.3963 \pm 0.0250)})$ with $R^2 = 0.9970$, which ascertains the reliability of the developed sensor over a broad dynamic range for applicability in glucose detection.

3.5. Selectivity, repeatability, reproducibility, and shelf-life of CuNP-ink/PDE

Selectivity, reproducibility, and stability of a biosensor are very

Table 2
Performance comparison of proposed CuNP-ink/PDE sensor with existing published works on non-enzymatic glucose sensors.

Electrode material	Sensitivity ($\mu AmM^{-1}cm^{-2}$)	Limit of detection (μM)	Response time (s)	Applied potential (V)	Reference
GP-MoS_2-Cu	3380	0.5	3	+0.42	[48]
CuO/LSG	–	0.1	< 0.2	+0.40	[49]
CuO-IL/rGO modified SPEC	–	0.14	20	–	[52]
CFP/GWs/Cu_2O	–	0.21	< 4	+0.55	[53]
Cu-xCu_2O NPs/3DG film	230.86	16	–	–	[69]
Cu nanoparticle/graphene/FTO	430	7.2	< 4	+0.65	[70]
CuO/ITO	450.2	0.7	–	+0.59	[71]
PEDOT:PSS-CuO-MWCNTs/PGE	663.2	0.23	–	+0.70	[72]
CuxOHM/RGO	635.3	1.15	–	+0.50	[73]
CuO MF-SPE	383	10	~2	+0.55	[74]
CuNP-ink/PDE	**2691.7**	**0.5**	**~1.5**	**+0.30**	**This work**

crucial in practical applications. Therefore, we have examined the influence of electrochemically active compounds, including 0.05 mM sucrose (Suc), 5 mM lactic acid (LA), 0.01 mM ascorbic acid (AA), 0.2 mM uric acid (UA), and 0.05 mM dopamine (DA), are present in human sweat [6]. From Fig. 4e, it is evident that 0.1 mM glucose shows a significant current response when compared with other interfering species, thus demonstrating a high selectivity towards glucose. This excellent selectivity is ascribed to the formation of partial surface oxide on the CuNP-ink/PDE that minimizes the effect of the interfering species such as AA, UA, and DA [58,66]. Moreover, the formation of surface oxide is attributed to 44.5% of Cu nanoparticles in the deposited CuNP-ink, as revealed from EDX analysis. Thus, the high selectivity of the sensor is ascribed to the collegial behavior of metallic Cu nanoparticles and partially formed CuO at the electrode surface.

The repeatability of the sensor is tested by conducting amperometry for 1 mM glucose. For that, three sensors ($n = 3$) are repeatedly subjected to single drop addition of 10 μL glucose with a consecutive interval of 2 h for a duration of 12 h. After each reading, the sensors are soaked with tissue paper and then allowed to dry for 2 h at room temperature until the next trial. From Fig. 4f it is observed that the response of the sensors degrades drastically and falls to 43% of the first reading which interprets poor repeatability of the sensor, thereby inducing a disposable nature to the sensor.

Fig. 4g shows the current response of ten separately fabricated sensors upon 1 mM glucose addition. The observed current in each consecutive glucose addition is 0.255 ± 0.0039 μA which signifies that the sensor offers reproducible results. Each sensor is meant for one-time measurement after which it is disposed of. Also, the relative standard deviation (RSD) for ten glucose measurements is found to be 1.56% which further affirms the high reproducibility of the developed sensor. The reason for such high reproducibility can be ascribed to uniform pencil drawing over the paper substrate by monitoring the hand force with a digital dynamometer and deposition of an equal amount of CuNP-ink and Ag-ink on the PDE. The applied force of the handwritten pencil sensor has already been experimented with to develop reproducible sensors such as in Refs. [67,68].

The shelf-life of the developed sensor is examined by studying the amperometric response of the four identical sensors with an interval of one week. The sensors are fabricated on the same day to examine the reactive life-span of deposited CuNP-ink. The current response of first sensor is studied for one-drop addition of 10 μL of 1 mM glucose addition after one week of fabrication. Meanwhile, the other three sensors are stored at room temperature in a clean glass petri dish. Subsequently, after next week, the response of the second sensor is studied for 1 mM glucose and so on. Meanwhile, the sensors are disposed after each measurement. It has been found that the response current of the fourth sensor is 91% of that of the first sensor (Fig. 4h) which shows a remarkable shelf-life of our sensor.

3.6. Glucose detection in real sweat samples

The evaluation of glucose in real sweat samples is conducted with the approval of the institutional ethical committee for collecting and using on-body human sweat for experimental purposes. 4 healthy subjects (male: 2, female: 2) with a mean age of 32 ± 5 years are recruited for the sample collection from the institution campus through email distribution and oral messages. Before sample collection, the subjects are requested to provide written consent for participating in the experimental study. The samples are collected during the evening session of the gymnasium at 7 p.m. with room temperature and relative humidity of the gymnasium room as 28^oC and 70% respectively. The subjects' forehead and arms are properly cleaned with alcohol swabs before the treadmill running session. Then the subjects are made to run on the treadmill for 20 min at 10 km/hr (Fig. 1b). After 20 min, clean cotton balls are used to soak the sweat from the forehead and arms of each subject and are squeezed into four clean glass centrifuge tubes to obtain four sweat samples. The amount of sweat collected from each subject ranges from 3 to 4 mL. In the laboratory, the collected sweat samples are filtered three times to get rid of impurity contamination during sweat collection (Fig. 1c). The filtered samples ($S1 - S4$) are then preserved in clean glass tubes at 21^oC. Before analyzing the sweat samples with our fabricated sensor, each sweat sample is diluted three times with 0.1 M NaOH under constant stirring. During the experimentation, each sweat sample is divided into three parts for a threefold validation to obtain precise glucose concentration measurements. The sweat samples are then evaluated with 12 sensors by performing amperometry at + 0.30 V. The current obtained from each sensor (Table S5) is correlated with the calibration curve (Fig. 4d) for estimating sweat glucose concentration ($Glu_{CuNP-ink/PDE}$).

To validate the performance of our sensor in measuring glucose in real sweat samples, a UV–Vis spectrophotometry assay has been used. The method adopted for glucose determination using UV–Vis spectrophotometer has been adopted from literature [75] and is discussed in Supplementary Information, Section S3. Initially, the absorbance of known glucose concentrations is measured by UV–Vis spectrophotometer at 575 nm wavelength (Table S6) and a calibration plot is obtained (Fig. S4). Then, the preserved sweat samples ($S1 - S4$) are examined by UV–Vis spectrophotometer at 575 nm wavelength using three-fold validation method to obtain the absorbance of each sample (Table S7). Using the calibration equation derived from the plot of Fig. S4, the concentration of each sweat sample is obtained (see Supplementary Information, Table S7). When compared, the glucose concentration estimated by using UV–Vis spectrophotometer and our sensors shows proximity between the measurements (Table 3). Fig. S5 shows the error-bar plot of the comparison. Thus the developed sensor shows promising performance in sweat glucose detection and has the potential to perform in real-world applications.

Table 3
Comparison of glucose concentration estimation in real human sweat samples of four subjects with the developed sensor with that of UV–Vis spectrophotometer results [$\overline{C_1}$ and $\overline{C_2}$ are the mean and σ represents the standard deviation from the respective mean.].

Volunteer	$Glu_{CuNP-ink/PDE}$	Glu_{UV-Vis}
	$(\overline{C_1} \pm \sigma)$ (mM)	$(\overline{C_2} \pm \sigma)$ (mM)
S1	0.4596 ± 0.0067	0.4695 ± 0.0032
S2	0.5813 ± 0.0091	0.5715 ± 0.0036
S3	0.2072 ± 0.0039	0.2195 ± 0.0018
S4	0.3895 ± 0.0058	0.3980 ± 0.0042

4. Conclusion

We have presented a very simple method of fabricating a glucose sensor by hand drawing a sensitive layer of copper nanoparticle ink over a pencil-drawn electrode on a Whatman filter paper substrate. The solution method of fabricating a sensitive layer using nanoparticle ink allows permeation of glucose-sensitive copper nanoparticles deep into the porous paper. Moreover, dispersion of ink relieves the inner stress of the deposited sensitive layer that provides good mechanical stability to the designed structure. The presence of metallic Cu nanoparticles in the deposited ink further promotes electro-oxidation of glucose in a strongly alkaline medium. Also, the formation of CuO on the electrode surface helps in nullifying the effect of interfering species present in sweat while measuring glucose. The sensor offers excellent sensitivity and low detection limit owing to the inherent nanostructure of the metallic Cu as well as large surface area which provide an outstanding electron transfer rate at the electrocatalytic junction. Besides, the sensor size of 25 mm×10 mm promotes the future work of developing a miniaturized electronic wearable platform for continuous glucose monitoring. Thus, the developed sensor is a seamless and affordable tool in terms of sweat glucose evaluation for effective utilization by the end-user.

CRediT authorship contribution statement

Amarprit Singh: Conceptualization, Data curation, is involved in the conception and design of the work reported, involved in conducting the experiments and collection of data, Formal analysis, Writing – original draft, All the authors contributed equally in the data analysis and interpretation. All the authors contributed equally in the drafting of article. **Anil Hazarika:** Data curation, Formal anlaysis, Writing - origianla draft, All the authors contributed equally in the data analysis and interpretation. All the authors contributed equally in the drafting of article. **Lachit Dutta:** Data curation, Formal analysis, Writing – original draft, All the authors contributed equally in the data analysis and interpretation. All the authors contributed equally in the drafting of article. **Abhishruti Bhuyan:** Data curation, Formal analysis, Writing – original draft, All the authors contributed equally in the data analysis and interpretation. All the authors contributed equally in the drafting of article. **Manabendra Bhuyan:** Data curation, Formal analysis, Writing – original draft, All the authors contributed equally in the data analysis and interpretation. All the authors contributed equally in the drafting of article, Supervision, The whole work is carried out at the Department of Electronics and Communication Engineering, Tezpur University (India), under the extreme supervision of Prof. Manabendra Bhuyan.

Declaration of competing interest

The authors declare the following financial interests/personal relationships which may be considered as potential competing interests: Amarprit Singh reports financial support was provided by Department of Science and Technology, Govt. of India.

Data availability

The authors do not have permission to share data.

Acknowledgment

The authors greatly thank the Department of Science and Technology, Government of India, for financial support in conducting this research work (Fund Sanction Order No. DST/INSPIRE Fellowship/2018/IF180845). The authors are also grateful to Mr. Arun K. Gupta, Department of Food Engineering and Technology, Tezpur University, for his assistance in real sweat sample evaluation.

Appendix A. Supplementary data

Supplementary data to this article can be found online at https://doi.org/10.1016/j.aca.2022.340257.

References

[1] J.B. Cole, J.C. Florez, Genetics of diabetes mellitus and diabetes complications, Nat. Rev. Nephrol. 16 (7) (2020) 377–390.
[2] T.K. Oser, M.L. Litchman, N.A. Allen, B.M. Kwan, L. Fisher, B.T. Jortberg, W. H. Polonsky, S.M. Oser, Personal continuous glucose monitoring use among adults with type 2 diabetes: clinical efficacy and economic impacts, Curr. Diabetes Rep. 21 (11) (2021) 1–16.
[3] D. Atlas, International Diabetes Federation, IDF Diabetes Atlas, seventh ed., 2015. Brussels, Belgium.
[4] E. Bihar, S. Wustoni, A.M. Pappa, K.N. Salama, D. Baran, S. Inal, A fully inkjet-printed disposable glucose sensor on paper, npj Flex. Electron. 2 (1) (2018) 1–8.
[5] N.O.S. Câmara, K. Iseki, H. Kramer, Z.H. Liu, K. Sharma, Kidney disease and obesity: epidemiology, mechanisms and treatment, Nat. Rev. Nephrol. 13 (3) (2017) 181–190.
[6] Y. Wang, X. Wang, W. Lu, Q. Yuan, Y. Zheng, B. Yao, A thin film polyethylene terephthalate (PET) electrochemical sensor for detection of glucose in sweat, Talanta 198 (2019) 86–92.
[7] A. Singh, A. Hazarika, C. Talukdar, M. Bhuyan, L. Dutta, M. Barthakur, K. Chakraborty, Microcontroller-based online nerve parameter estimation for diagnosis of healthy subject using real-time nerve conduction study signal acquired using voltage controlled neurostimulator, IEEE Trans. Ind. Inf. 17 (11) (2021) 7546–7553.
[8] D. Olczuk, R. Priefer, A history of continuous glucose monitors (CGMs) in self-monitoring of diabetes mellitus, Diabetes Metab. 12 (2) (2018) 181–187.
[9] A. Bhide, S. Muthukumar, A. Saini, S. Prasad, Simultaneous lancet-free monitoring of alcohol and glucose from low-volumes of perspired human sweat, Sci. Rep. 8 (1) (2018) 1–11.
[10] P. Ramadoss, M.I. Rahman, A. Perumal, R. Nallaiyan, S.H. Basha, A. Dakshanamoorthy, Non-invasive, non-enzymatic, biodegradable and flexible sweat glucose sensor and its electrochemical studies, ChemistrySelect 5 (36) (2020) 11305–11321.
[11] J. Moyer, D. Wilson, I. Finkelshtein, B. Wong, R. Potts, Correlation between sweat glucose and blood glucose in subjects with diabetes, Diabetes Technol. Therapeut. 14 (5) (2012) 398–402.
[12] A. Alizadeh, A. Burns, R. Lenigk, R. Gettings, J. Ashe, A. Porter, M. McCaul, R. Barrett, D. Diamond, P. White, P. Skeath, A wearable patch for continuous monitoring of sweat electrolytes during exertion, Lab Chip 18 (17) (2018) 2632–2641.
[13] H. Lee, C. Song, Y.S. Hong, M.S. Kim, H.R. Cho, T. Kang, K. Shin, S.H. Choi, T. Hyeon, D.H. Kim, Wearable/disposable sweat-based glucose monitoring device with multistage transdermal drug delivery module, Sci. Adv. 3 (3) (2017), e1601314.
[14] G. Xu, C. Cheng, Z. Liu, W. Yuan, X. Wu, Y. Lu, S.S. Low, J. Liu, L. Zhu, D. Ji, S. Li, Battery-free and wireless epidermal electrochemical system with all-printed stretchable electrode array for multiplexed in situ sweat analysis, Adv. Mater. Technol. 4 (7) (2019), 1800658.
[15] Y. Lei, W. Zhao, Y. Zhang, Q. Jiang, J.H. He, A.J. Baeumner, O.S. Wolfbeis, Z. L. Wang, K.N. Salama, H.N. Alshareef, A MXene-based wearable biosensor system for high-performance in vitro perspiration analysis, Small 15 (19) (2019), 1901190.
[16] H.Y.Y. Nyein, L.C. Tai, Q.P. Ngo, M. Chao, G.B. Zhang, W. Gao, M. Bariya, J. Bullock, H. Kim, H.M. Fahad, A. Javey, A wearable microfluidic sensing patch for dynamic sweat secretion analysis, ACS Sens. 3 (5) (2018) 944–952.
[17] Y. Chen, S. Lu, S. Zhang, Y. Li, Z. Qu, Y. Chen, B. Lu, X. Wang, X. Feng, Skin-like biosensor system via electrochemical channels for noninvasive blood glucose monitoring, Sci. Adv. 3 (12) (2017), e1701629.
[18] A.J. Bandodkar, W. Jia, C. Yardımcı, X. Wang, J. Ramirez, J. Wang, Tattoo-based noninvasive glucose monitoring: a proof-of-concept study, Anal. Chem. 87 (1) (2015) 394–398.
[19] H.Y.Y. Nyein, W. Gao, Z. Shahpar, S. Emaminejad, S. Challa, K. Chen, H.M. Fahad, L.C. Tai, H. Ota, R.W. Davis, A. Javey, A wearable electrochemical platform for

noninvasive simultaneous monitoring of Ca^{2+} and pH, ACS Nano 10 (7) (2016) 7216–7224.
[20] J. Park, Y. Jeong, J. Kim, J. Gu, J. Wang, I. Park, Biopsy needle integrated with multi-modal physical/chemical sensor array, Biosens. Bioelectron. 148 (2020), 111822.
[21] C.L. Choong, M.B. Shim, B.S. Lee, S. Jeon, D.S. Ko, T.H. Kang, J. Bae, S.H. Lee, K. E. Byun, J. Im, Y.J. Jeong, Highly stretchable resistive pressure sensors using a conductive elastomeric composite on a micropyramid array, Adv. Mater. 26 (21) (2014) 3451–3458.
[22] J.R. Sempionatto, A.A. Khorshed, A. Ahmed, A.N. De Loyola e Silva, A. Barfidokht, L. Yin, K.Y. Goud, M.A. Mohamed, E. Bailey, J. May, C. Aebischer, Epidermal enzymatic biosensors for sweat vitamin C: toward personalized nutrition, ACS Sens. 5 (6) (2020) 1804–1813.
[23] J. Liu, X. Jiang, R. Zhang, Y. Zhang, L. Wu, W. Lu, J. Li, Y. Li, H. Zhang, MXene-enabled electrochemical microfluidic biosensor: applications toward multicomponent continuous monitoring in whole blood, Adv. Funct. Mater. 29 (6) (2019), 1807326.
[24] Y. Liu, M. Pharr, G.A. Salvatore, Lab-on-skin: a review of flexible and stretchable electronics for wearable health monitoring, ACS Nano 11 (10) (2017) 9614–9635.
[25] A.W. Martinez, S.T. Phillips, M.J. Butte, G.M. Whitesides, Patterned paper as a platform for inexpensive, low-volume, portable bioassays, Angew. Chem. 119 (8) (2007) 1340–1342.
[26] T. Akyazi, L. Basabe-Desmonts, F. Benito-Lopez, Review on microfluidic paper-based analytical devices towards commercialisation, Anal. Chim. Acta 1001 (2018) 1–17.
[27] D.A. Bruzewicz, M. Reches, G.M. Whitesides, Low-cost printing of poly (dimethylsiloxane) barriers to define microchannels in paper, Anal. Chem. 80 (9) (2008) 3387–3392.
[28] H. Shibata, Y. Hiruta, D. Citterio, Fully inkjet-printed distance-based paper microfluidic devices for colorimetric calcium determination using ion-selective optodes, Analyst 144 (4) (2019) 1178–1186.
[29] T. Akyazi, A. Tudor, D. Diamond, L. Basabe-Desmonts, L. Florea, F. Benito-Lopez, Driving flows in microfluidic paper-based analytical devices with a cholinium based poly (ionic liquid) hydrogel, Sensor. Actuator. B Chem. 261 (2018) 372–378.
[30] Y. He, Y. Wu, J.Z. Fu, W.B. Wu, Fabrication of paper-based microfluidic analysis devices: a review, RSC Adv. 5 (95) (2015) 78109–78127.
[31] M.M. Bordbar, A. Sheini, P. Hashemi, A. Hajian, H. Bagheri, Disposable paper-based biosensors for the point-of-care detection of hazardous contaminations-A review, Biosensors 11 (9) (2021) 316.
[32] J. Kim, D. Ahn, J. Sun, S. Park, Y. Cho, S. Park, S. Ha, S. Ahn, Y.A. Kim, J.J. Park, Vertically and horizontally drawing formation of graphite pencil electrodes on paper by frictional sliding for a disposable and foldable electronic device, ACS Omega 6 (3) (2020) 1960–1970.
[33] E.Y. Jomma, N. Bao, S.N. Ding, A pencil drawn microelectrode on paper and its application in two-electrode electrochemical sensors, Anal. Methods 9 (23) (2017) 3513–3518.
[34] N. Kurra, G.U. Kulkarni, Pencil-on-paper: electronic devices, Lab Chip 13 (15) (2013) 2866–2873.
[35] N. Dossi, R. Toniolo, A. Pizzariello, F. Impellizzieri, E. Piccin, G. Bontempelli, Pencil-drawn paper supported electrodes as simple electrochemical detectors for paper-based fluidic devices, Electrophoresis 34 (14) (2013) 2085–2091.
[36] Q. Hua, H. Liu, J. Zhao, D. Peng, X. Yang, L. Gu, C. Pan, Bioinspired electronic whisker arrays by pencil-drawn paper for adaptive tactile sensing, Adv. Electron. Mater. 2 (7) (2016), 1600093.
[37] K.C. Honeychurch, The voltammetric behaviour of lead at a hand drawn pencil electrode and its trace determination in water by stripping voltammetry, Anal. Methods 7 (6) (2015) 2437–2443.
[38] X. Strakosas, J. Selberg, P. Pansodtee, N. Yonas, P. Manapongpun, M. Teodorescu, M. Rolandi, A non-enzymatic glucose sensor enabled by bioelectronic pH control, Sci. Rep. 9 (1) (2019) 1–7.
[39] A. Rahim, Z.U. Rehman, S. Mir, N. Muhammad, F. Rehman, M.H. Nawaz, M. Yaqub, S.A. Siddiqi, A.A. Chaudhry, A non-enzymatic glucose sensor based on CuO-nanostructure modified carbon ceramic electrode, J. Mol. Liq. 248 (2017) 425–431.
[40] S. Pourbeyram, K. Mehdizadeh, Nonenzymatic glucose sensor based on disposable pencil graphite electrode modified by copper nanoparticles, J. Food Drug Anal. 24 (4) (2016) 894–902.
[41] P. Lv, H. Zhou, A. Mensah, Q. Feng, D. Wang, X. Hu, Y. Cai, L.A. Lucia, D. Li, Q. Wei, A highly flexible self-powered biosensor for glucose detection by epitaxial deposition of gold nanoparticles on conductive bacterial cellulose, Chem. Eng. J. 351 (2018) 177–188.
[42] J. Ryu, K. Kim, H.S. Kim, H.T. Hahn, D. Lashmore, Intense pulsed light induced platinum–gold alloy formation on carbon nanotubes for non-enzymatic glucose detection, Biosens. Bioelectron. 26 (2) (2010) 602–607.
[43] E. Sehit, Z. Altintas, Significance of nanomaterials in electrochemical glucose sensors: an updated review (2016-2020), Biosens. Bioelectron. 159 (2020), 112165.
[44] X. Zhang, G. Wang, W. Zhang, Y. Wei, B. Fang, Fixure-reduce method for the synthesis of Cu_2O/MWCNTs nanocomposites and its application as enzyme-free glucose sensor, Biosens. Bioelectron. 24 (11) (2009) 3395–3398.
[45] J.W. Wu, C.H. Wang, Y.C. Wang, J.K. Chang, Ionic-liquid-enhanced glucose sensing ability of non-enzymatic Au/graphene electrodes fabricated using supercritical CO_2 fluid, Biosens. Bioelectron. 46 (2013) 30–36.
[46] H.X. Wu, W.M. Cao, Y. Li, G. Liu, Y. Wen, H.F. Yang, S.P. Yang, In situ growth of copper nanoparticles on multiwalled carbon nanotubes and their application as non-enzymatic glucose sensor materials, Electrochim. Acta 55 (11) (2010) 3734–3740.
[47] Z. Lin, G. Wu, L. Zhao, K.W.C. Lai, Carbon nanomaterial-based biosensors: a review of design and applications, IEEE Nanotechnol. Mag. 13 (5) (2019) 4–14.
[48] Z. Wang, S. Dong, M. Gui, M. Asif, W. Wang, F. Wang, H. Liu, Graphene paper supported MoS_2 nanocrystals monolayer with Cu submicron-buds: high-performance flexible platform for sensing in sweat, Anal. Biochem. 543 (2018) 82–89.
[49] A. Prabhakaran, P. Nayak, Surface engineering of laser-scribed graphene sensor enables non-enzymatic glucose detection in human body fluids, ACS Appl. Nano Mater. 3 (1) (2019) 391–398.
[50] I.H. Yeo, D.C. Johnson, Anodic response of glucose at copper-based alloy electrodes, J. Electroanal. Chem. 484 (2) (2000) 157–163.
[51] M.B. Gawande, A. Goswami, F.X. Felpin, T. Asefa, X. Huang, R. Silva, X. Zou, R. Zboril, R.S. Varma, Cu and Cu-based nanoparticles: synthesis and applications in catalysis, Chem. Rev. 116 (6) (2016) 3722–3811.
[52] N. Janmee, P. Preechakasedkit, N. Rodthongkum, O. Chailapakul, P. Potiyaraj, N. Ruecha, A non-enzymatic disposable electrochemical sensor based on surface-modified screen-printed electrode CuO-IL/rGO nanocomposite for a single-step determination of glucose in human urine and electrolyte drinks, Anal. Methods 13 (25) (2021) 2796–2803.
[53] H. Yang, J. Bao, Y. Qi, J. Zhao, Y. Hu, W. Wu, X. Wu, D. Zhong, D. Huo, C. Hou, A disposable and sensitive non-enzymatic glucose sensor based on 3D graphene/Cu_2O modified carbon paper electrode, Anal. Chim. Acta 1135 (2020) 12–19.
[54] K. Justice Babu, S. Sheet, Y.S. Lee, G. Gnana Kumar, Three-dimensional dendrite Cu–Co/reduced graphene oxide architectures on a disposable pencil graphite electrode as an electrochemical sensor for nonenzymatic glucose detection, ACS Sustain. Chem. Eng. 6 (2) (2018) 1909–1918.
[55] P.K. Khanna, S. Gaikwad, P.V. Adhyapak, N. Singh, R. Marimuthu, Synthesis and characterization of copper nanoparticles, Mater. Lett. 61 (25) (2017) 4711–4714.
[56] Silver Conductive Pen 842AR-P Technical Data Sheet.
[57] J. Luo, S. Jiang, H. Zhang, J. Jiang, X. Liu, A novel non-enzymatic glucose sensor based on Cu nanoparticle modified graphene sheets electrode, Anal. Chim. Acta 709 (2012) 47–53.
[58] Y. Zhang, L. Su, D. Manuzzi, H.V.E. de los Monteros, W. Jia, D. Huo, C. Hou, Y. Lei, Ultrasensitive and selective non-enzymatic glucose detection using copper nanowires, Biosens. Bioelectron. 31 (1) (2012) 426–432.
[59] J.M. Marioli, T. Kuwana, Electrochemical characterization of carbohydrate oxidation at copper electrodes, Electrochim. Acta 37 (7) (1992) 1187–1197.
[60] Y. Zhang, N. Li, Y. Xiang, D. Wang, P. Zhang, Y. Wang, S. Lu, R. Xu, J. Zhao, A flexible non-enzymatic glucose sensor based on copper nanoparticles anchored on laser-induced graphene, Carbon 156 (2020) 506–513.
[61] N. Karikalan, R. Karthik, S.M. Chen, H.A. Chen, A voltammetric determination of caffeic acid in red wines based on the nitrogen doped carbon modified glassy carbon electrode, Sci. Rep. 7 (1) (2017) 1–10.
[62] S.R. Balakrishnan, U. Hashim, G.R. Letchumanan, M. Kashif, A.R. Ruslinda, W. W. Liu, P. Veeradasan, R.H. Prasad, K.L. Foo, P. Poopalan, Development of highly sensitive polysilicon nanogap with APTES/GOx based lab-on-chip biosensor to determine low levels of salivary glucose, Sens. Actuator A Phys. 220 (2014) 101–111.
[63] X. Liao, Q. Liao, X. Yan, Q. Liang, H. Si M. Li, H. Wu, S. Cao, Y. Zhang, Flexible and highly sensitive strain sensors fabricated by pencil drawn for wearable monitor, Adv. Funct. Mater. 25 (16) (2015) 2395–2401.
[64] M. Carbone, L. Gorton, R. Antiochia, An overview of the latest graphene-based sensors for glucose detection: the effects of graphene defects, Electroanalysis 27 (1) (2015) 16–31.
[65] E. Turiel, C. Perez-Conde, A. Martin-Esteban, Assessment of the cross-reactivity and binding sites characterisation of a propazine-imprinted polymer using the Langmuir-Freundlich isotherm, Analyst 128 (2) (2003) 137–141.
[66] L.C. Jiang, W.D. Zhang, A highly sensitive nonenzymatic glucose sensor based on CuO nanoparticles-modified carbon nanotube electrode, Biosens. Bioelectron. 25 (6) (2010) 1402–1407.
[67] J. Zhang, L. Huang, Y. Lin, L. Chen, Z. Zeng, L. Shen, Q. Chen, W. Shi, Pencil-trace on printed silver interdigitated electrodes for paper-based NO_2 gas sensors, Appl. Phys. Lett. 106 (14) (2015), 143101.
[68] W. Li, D. Qian, Q. Wang, Y. Li, N. Bao, H. Gu, C. Yu, Fully-drawn origami paper analytical device for electrochemical detection of glucose, Sensor. Actuator. B Chem. 231 (2016) 230–238.
[69] Z. Khosroshahi, F. Karimzadeh, M. Kharaziha, A. Allafchian, A non-enzymatic sensor based on three-dimensional graphene foam decorated with Cu-xCu_2O nanoparticles for electrochemical detection of glucose and its application in human serum, Mater. Sci. Eng. C 108 (2020), 110216.
[70] T. Soganci, R. Ayranci, E. Harputlu, K. Ocakoglu, M. Acet, M. Farle, C.G. Unlu, M. Ak, An effective nonenzymatic biosensor platform based on copper nanoparticles decorated by sputtering on CVD graphene, Sensor. Actuator. B Chem. 273 (2018) 1501–1507.
[71] T. Wang, W. Su, Y. Fu, J. Hu, Controllably annealed CuO-nanoparticle modified ITO electrodes: characterisation and electrochemical studies, Appl. Surf. Sci. 390 (2016) 795–803.
[72] Z. Amirzadeh, S. Javadpour, M.H. Shariat, R. Knibbe, Non-enzymatic glucose sensor based on copper oxide and multi-wall carbon nanotubes using PEDOT: PSS matrix, Synth. Met. 245 (2018) 160–166.
[73] F. Zhang, S. Huang, Q. Guo, H. Zhang, H. Li, Y. Wang, J. Fu, X. Wu, L. Xu, M. Wang, One-step hydrothermal synthesis of Cu_2O/CuO hollow microspheres/reduced

graphene oxide hybrid with enhanced sensitivity for non-enzymatic glucose sensing, Colloids Surf. A Physicochem. Eng. 602 (2020), 125076.
[74] B.G. Mahmoud, M. Khairy, F.A. Rashwan, C.W. Foster, C.E. Banks, Self-assembly of porous copper oxide hierarchical nanostructures for selective determinations of glucose and ascorbic acid, RSC Adv. 6 (18) (2016) 14474–14482.
[75] G.L. Miller, Use of dinitrosalicylic acid reagent for determination of reducing sugar, Anal. Chem. 31 (3) (1959) 426–428.